2023 3rd International Conference on Electrical Machines and Drives (ICEMD), 20-21 December 2023, Tehran, Iran.

Torque Ripple reduction of BLDC Motor Drive using Finite-Control-Set Model Predictive Control Strategy

Zahra Emami
Dept. of Electrical & Computer Eng.
University of Kashan
Kashan, Iran
zahra_emami1765@yahoo.com

Abolfazl Halvaei Niasar
Dept. of Electrical & Computer Eng.
University of Kashan
Kashan, Iran
halvaei@kashanu.ac.ir

2023 3rd International Conference on Electrical Machines and Drives (ICEMD) | 979-8-3503-9374-3/23/$31.00 ©2023 IEEE | DOI: 10.1109/ICEMD60816.2023.10429610

Abstract*—Brushless DC (BLDC) motor is the first option for lightweight industrial application and electric vehicles because of its high power density and high torque and low maintenance and suitable speed range. The vehicle environment is very dynamic, nonlinear, and noisy. This paper has investigated comparative research between two control strategy of BLDC motors: The speed control strategy applying a model predictive control (MPC) and BLDC motor stator current control method applying hysteresis current controllers. Suggested MPC strategy does not require Hall sensors and applies position sensor for gaining the back-EMF waveforms. The both methods were studied and simulated with the same working conditions. Also, qualitative and quantitative analyzes were performed for both methods and the results of both methods were obtained. The simulations in MATLAB-SIMULINK show that the target control method of the predictive model works better than the hysteresis current control method in terms of torque and following the reference speed.

Keywords—BLDC motor; Back-EMF; Hall sensor, torque model predictive control; hysteresis current controller.

I. INTRODUCTION

Brushless DC (BLDC) motor drive have the superiority of high efficiency, high power density Compared to PMSM motors. This superiority cause BLDC motor drive be extensively used in Industrial and electrical vehicle (EV) applications [1][2]. Simple structure, good speed torque characteristics in a wide speed range and high power-to-volume ratio which makes them capable of producing higher torque and power than PMSM motors. This feature is important for motors used in vehicle electrical and electrical household appliances. But, these motors face problems such as torque ripple at the moment of commutation, which researchers are looking for to solve this problem. Therefore, today, reducing torque ripple and improving their performance has become a significant issue for researchers [3] [4] [5]. As the torque ripple increases, mechanical stress and acoustic noise increase and efficiency decreases [6] [7].

Different control strategies have been suggested for BLDC motors [7] [8]. These strategies include: dc link current control, direct torque control (DTC) in [9], field-oriented control (FOC) and space vector control.

In recent years, the predictive strategy for all kinds of electric motors and electric converters is growing and developing rapidly [7] [10][11]. In the Model Predictive Control (MPC) method, the future performance of the system is predicted for a limited period of time, and according to that, optimal control is performed in the future for the objective function defined in the system optimal states are applied to the system [12][13].

A BLDC motor drive with MPC control scheme is appropriate for less price and better performance structure, have presented in this work. A hysteresis current control strategy applying hysteresis current controllers is still used as a widely used method, his method is used in various motors such as PMSMs and induction motors and because of low cost and the simple practical implementation. This method uses of the relation between torque and motor current [15].

Today, various high speed DSPs hardware such as hardware in the loop has provided the implementation of complex algorithms for control boards in electric motor drives. Thus, various control strategies have been promoted to improve control of BLDC motor drives. However, applying this technique to a BLDC motor without Hall effect sensor BLDC motor has not been discussed so far. This strategy used is the finite control set model predictive control approach (FCS-MPC) [16].

This paper considers to investigate a different and new method for driving BLDC motor based on model predictive control. This method does not require Hall sensors and uses position sensor for gaining the values of back-EMF waveforms. The suggested control method has less torque ripple than the traditional current control method. In addition to, traditional hysteresis method has been described and has been compared with new method. The traditional hysteresis current control method uses of Hall sensors to measure phase currents [17].

The rest of the article includes the following sections: Section II expresses the model of mathematical BLDC motor and inverter system configuration. Section III describes the suggesteded model predictive control plan. In Section IV, Simulation has been done in different control modes and discussion and analysis have been done. Also, At the end of the article, a conclusion is drawn from the simulations.

Simulations have done using MATLAB-Simulink that assesses the possibility of practical implementation of the suggested method for a low-power BLDC motor. The suggested method is compared with the traditional method and

provides less torque ripple. At first, the suggested controller predicts the future value of the motor torque in finite time frame. Then obtained value is compared with reference torque that has generated by the speed controller.

II. Configuration and Model of the BLDC Motor

Fig. 1 shows equivalent circuit of the BLDC motor which is simply state where the phase stator winding resistance is demonstrated by (R_s) and the phase inductance is represented by (L_s). Also, the mutual inductance between each phase is displayed by (M). Every phase back-EMFs (e_a, e_b, e_c) are trapezoidal in the case of one ideal BLDC motor. All three back-EMFs have a phase difference of 120 degrees to one another .The system drive is done using a three-phase inverter that including six switches.

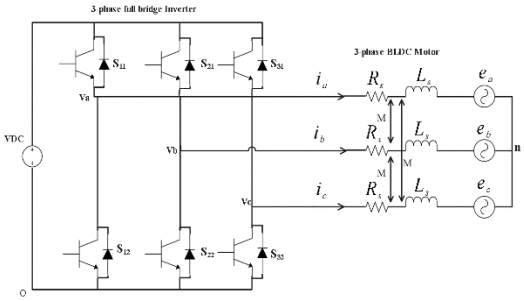

Fig. 1. Equivalent model of the BLDC motor drived by a three phase inverter.

The mathematical model of the motor including the terminal voltage equations of three phases an, bn, cn and back-EMFs are given separately with the following relations:

$$V_{an} = R_a i_a + \frac{d}{dt}(L_a i_a + M_{ab} i_b + M_{ac} i_c) + e_a$$
$$V_{bn} = R_b i_b + \frac{d}{dt}(L_b i_b + M_{ba} i_a + M_{bc} i_c) + e_b \quad (1)$$
$$V_{cn} = R_c i_c + \frac{d}{dt}(L_c i_c + M_{ca} i_a + M_{cb} i_b) + e_c$$

Based on the fact that the motor never saturates, and iron losses ignore. Also, assuming that the elements of one phase are similar to another phase. According to these assumptions, equation (2) can be whitened, which is equivalent to model BLDC motor.

$$\begin{bmatrix} V_{an} \\ V_{bn} \\ V_{cn} \end{bmatrix} = \begin{bmatrix} R_s & 0 & 0 \\ 0 & R_s & 0 \\ 0 & 0 & R_s \end{bmatrix} \begin{bmatrix} i_a \\ i_b \\ i_c \end{bmatrix} + \begin{bmatrix} L_s - M & 0 & 0 \\ 0 & L_s - M & 0 \\ 0 & 0 & L_s - M \end{bmatrix} \frac{d}{dt} \begin{bmatrix} i_a \\ i_b \\ i_c \end{bmatrix} + \begin{bmatrix} e_a \\ e_b \\ e_c \end{bmatrix} \quad (2)$$

As mentioned, back-EMFs in an ideal BLDC motor are trapezoidal and have a phase difference of 120 degrees. For trapezoidal back-EMFs of one BLDC motor, the following EMFs is expressed as:

$$e_a = k_e \omega_m f_a(\theta_e)$$
$$e_b = k_e \omega_m f_b(\theta_e) \quad (3)$$
$$e_c = k_e \omega_m f_c(\theta_e)$$

Where ω_m is the mechanical speed in rad/s and k_e is the back-EMF constant and $f_a(\theta_e)$, $f_b(\theta_e)$ and $f_c(\theta_e)$ are three-phase trapezoidal back-EMFs functions that have same magnitude that is illustrated in Fig. 2 [7].

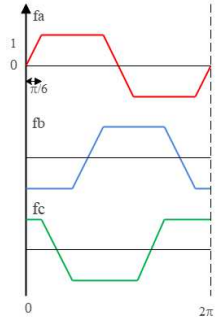

Fig. 2. Three-phase trapezoidal back-EMF functions.

The relationship between motor electromagnetic torque and rotor speed is according to equation (4). The electromagnetic torque BLDC motor is used to drive the mechanical load and dominate motor mechanical friction and inertia of BLDC motor within the speed acceleration [7]:

$$T_e = T_L + J\frac{d}{dt}\omega_m + B\omega_m \quad (4)$$

T_L is the load torque J is the inertia T_e is the electromagnetic torque and B demonstrates the mechanical friction.

Another electromagnetic torque relationship that can be written for BLDC motor is the relationship between current, back-EMF and torque which is expressed as follows:

$$T_e = T_a + T_b + T_c = \frac{(e_a i_a + e_b i_b + e_c i_c)}{\omega_m} \quad (5)$$

III. The Suggested Control Strategy

In strategy BLDC motor control, Hall effect sensor is removed and is used the position sensor for gaining the values of the back-EMF waveforms. Block diagram of traditional hysteresis current controller and the suggested predictive model control strategy without Hall sensor have shown in Fig. 3a and Fig. 3b. The traditional hysteresis current controller uses of hysteresis band. The current measured in each phase is compared with the reference current which creates an error. Controller aims the rotor speed follows the reference speed by compelling current in each phase that equalize with reference phase current.

The finite-control-set model predictive control (FCS-MPC) has fast dynamic response and simple implementation for control system optimization. Thus, MPC algorithm with a three-phase inverter with six-switch used in BLDC motor in Fig. 3b has shown. The block diagram of the suggested control system is illustrated in Fig. 3b. The proposed predictive control system includes three basis parts: Part (I) Speed control loop and torque generation; part (II) the MPC method and part (III) calculations including of values of back-EMFs, stator currents and voltage and torque in the stationary reference frame.

.

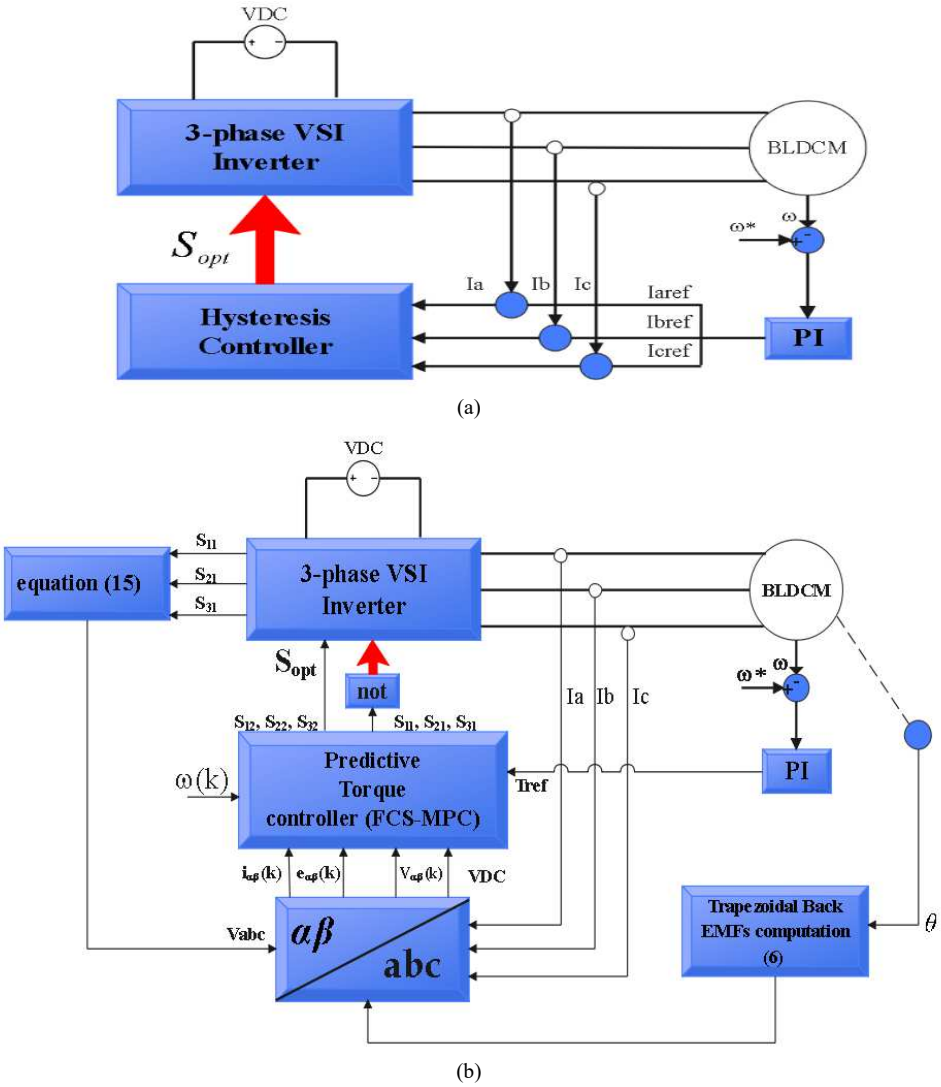

Fig. 3. The block diagram (a) traditional hystersis current controller, (b) suggested MPC

The MPC control part must calculate voltages of the back-EMF in each phase. The motor back-EMF voltages are calculated utilizing equations (6). In this method, motor back-EMF voltages do not use Hall sensors for measuring phase currents and the position sensor is used for obtaining the values of the back-EMF. The cosine waveforms are cut on E and -E and trapezoidal waveforms are obtained, which are the back-EMFs given by the following equation:

$$e_a = -0.9\mathrm{E} \le \cos\theta_e \le 0.9E$$
$$e_b = -0.9\mathrm{E} \le \cos(\theta_e - \tfrac{2\pi}{3}) \le 0.9E \quad (6)$$
$$e_c = -0.9\mathrm{E} \le \cos(\theta_e + \tfrac{2\pi}{3}) \le 0.9E$$

In equation (7), E is amplitude of back-EMF and ω_e rotor electrical position is defined as:

$$E = \lambda_m \omega_e \quad (7)$$

Where λ_m is linkage flux that its value 0.078115 and ω_e is:

$$\omega_e = \frac{p}{2}\omega_m \quad (8)$$

$$\theta_e = \frac{P}{2}\theta_m \quad (9)$$

In the above relation P, θ_e and θ_m are the number of rotor poles, rotor electrical position and rotor mechanical position respectively.

αβ stationary reference frame are used for voltage and current calculations. Thus, calculated back-EMF and voltages must transform to the αβ reference. Equation (10) shows the Clark transformation.

$$T = \frac{2}{3}\begin{bmatrix} 1 & -\frac{1}{2} & -\frac{1}{2} \\ 0 & \frac{\sqrt{3}}{2} & \frac{-\sqrt{3}}{2} \end{bmatrix} \quad (10)$$

A. The switching states of three-phase inverter

Accordingly, to equation (1), output voltage of three phase inverter is measured and calculated. The output voltage value of three phase inverter is obtained by using the inverter switching states and the DC link voltage. Because The target method works in three-phase conduction mode. Thus, switching states and voltage values obtains in in three-phase conduction mode with According to the Table I.

There are eight switching states in the three-phase conduction mode that is presented in Table I. Two the switches in the same leg aren't turned on at the identical time, because it creates a short circuit. Thus, the two switches in the one leg is complementary in accordance with equation (11).

TABLE I. THE SWITCHING STATES MODE SIX SWITCH THREE-PHASE INVERTER IN THE 3-PHASE CONDUCTION

S11	0	0	0	0	1	1	1	1
S21	0	0	1	1	0	0	1	1
S31	0	1	0	1	0	1	0	1
$\boldsymbol{V_{ab}}$	0	0	$-V_{DC}$	$-V_{DC}$	V_{DC}	V_{DC}	0	0
$\boldsymbol{V_{bc}}$	0	$-V_{DC}$	V_{DC}	0	0	$-V_{DC}$	V_{DC}	0
$\boldsymbol{V_{ca}}$	0	V_{DC}	0	$-V_{DC}$	$-V_{DC}$	0	$-V_{DC}$	0

$$S_{11} + S_{12} = 1$$
$$S_{21} + S_{22} = 1 \quad (11)$$
$$S_{31} + S_{32} = 1$$

Ac output line voltages obtains by using the following relations:

$$\frac{V_{DC}}{2}(S_{11} - S_{12}) = V_{an} + V_{no}$$
$$\frac{V_{DC}}{2}(S_{21} - S_{22}) = V_{bn} + V_{no} \quad (12)$$
$$\frac{V_{DC}}{2}(S_{31} - S_{32}) = V_{bn} + V_{no}$$

Adding the Equations (12) together gives Equation as:

$$\frac{V_{DC}}{2}(S_{11} + S_{21} + S_{31} - S_{12} - S_{22} - S_{32}) = V_{an} + V_{bn} + V_{cn} + 3V_{no} \quad (13)$$

Due to balanced voltages $V_{an} + V_{bn} + V_{cn} = 0$

$$\frac{V_{DC}}{6}(2S_{11} + 2S_{21} + 2S_{31} - 3) = V_{no} \quad (14)$$

Substituting V_{no} in Equation (12), the phase voltages are expressed as:

$$\frac{V_{DC}}{3}(2S_{11} - S_{21} - S_{31}) = V_{an}$$
$$\frac{V_{DC}}{3}(2S_{21} - S_{21} - S_{31}) = V_{bn} \quad (15)$$
$$\frac{V_{DC}}{3}(2S_{31} - S_{21} - S_{11}) = V_{cn}$$

It should be noted that only three up switches are used to calculate the voltage of the phases and down switches become negative and the optimal switching status is selected.

Measured and ccalculated phase voltages are transformed to the αβ reference according to the following equation:

$$\begin{bmatrix} v_{s\alpha} \\ v_{s\beta} \end{bmatrix} = T \begin{bmatrix} V_{an} \\ V_{bn} \\ V_{cn} \end{bmatrix} \quad (16)$$

Equation (2) is rewritten in αβ form by using of equation (16) and equation (17) is obtained:

$$\begin{bmatrix} v_{s\alpha} \\ v_{s\beta} \end{bmatrix} = \begin{bmatrix} R_s & 0 \\ 0 & R_s \end{bmatrix} \begin{bmatrix} i_\alpha \\ i_\beta \end{bmatrix} + \begin{bmatrix} L & 0 \\ 0 & L \end{bmatrix} \frac{d}{dt} \begin{bmatrix} i_\alpha \\ i_\beta \end{bmatrix} + \begin{bmatrix} e_\alpha \\ e_\beta \end{bmatrix} \quad (17)$$

The forward Euler method is applied to transform the continuous state of equation (17) to the discrete state of equation (19). Thus, the Euler approximation could be used as:

$$\frac{\mathrm{dx}}{\mathrm{dt}} = \frac{\mathrm{x(k+1)-x(k)}}{\mathrm{T_s}} \quad (18)$$

For predicting the value of variables during the next sample could be used the Euler approximation:

$$\frac{\mathrm{dx}}{\mathrm{dt}} = \frac{\mathrm{x(k+1)-x(k)}}{\mathrm{T_s}} \quad (18)$$

Where T_s is the sampling time x is the control variable. By writing the discrete equations of the BLDC drive and expressing the model in a discrete state, the MPC algorithm forecasts the future torque of BLDC motor based on the next value which sampled and cost function is used for optimization and optimal switching states selection.

By applying this approximation to equation (17) and equation (18), the following equations could be achieved:

$$\begin{bmatrix} i_\alpha(k+1) \\ i_\beta(k+1) \end{bmatrix} = \frac{T_s}{L_s}\left(\begin{bmatrix} v_{s\alpha}(k) \\ v_{s\beta}(k) \end{bmatrix} - \begin{bmatrix} e_\alpha(k) \\ e_{\beta(k)} \end{bmatrix}\right) + (1 - R_s \frac{T_s}{L_s}) \begin{bmatrix} i_\alpha(k) \\ i_{\beta(k)} \end{bmatrix} \quad (19)$$

The predicted torque of equation (20) is described based on predicted current of equation (19) and back-EMFs equation (6):

$$T_e(k+1) = \frac{3}{2}(e_\alpha(k) * I_\alpha(k+1) + e_\beta(k) * I_\beta(k+1))/\omega_m \quad (20)$$

B. Formulation of the Cost Function

The goal of the predicted method is to equalizing the value of $T_e(k+1)$ with the value of torque reference. The rotor speed is measured and compared to the value of speed reference and generates the value of reference torque and the created error passes by a PI controller, as indicated in Fig. 3b. T_{eref} represents the magnitude of the reference torque.

By applying the forecasted torque to function of cost, the optimal switching status are calculated and are applied to system. Function of cost of the suggested MPC is expressed as:

$$g=|T_{eref} - T_e(k+1)| \quad (21)$$

IV. SIMULATION AND ANALYSIS

In Fig. 3b, the simulation model of the BLDC motor drive is shown including of a six-switch three-phase inverter, suggested MPC control system and a BLDC motor is developed in software MATLAB-Simulink. Table II shows the case study system specifications. Speed waveform of the simulated suggested strategy and traditional strategy with fixed torque has displayed in Figures 4a and 4b. It is clear from the figures that the motor speed follows the reference speed in both of control strategy. Reference speed increases from 150 rpm and reaches 300 rpm at moment of 0.05 s. As it is seen, the speed controller error in the traditional hysteresis controller is 4%. But, this error in the predictive controller has decreased about1%. Zoomed of the rotor speed has been shown in Fig. 6c and 6d s in both of two methods.

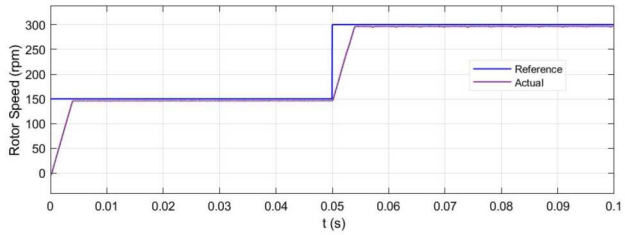

(a)

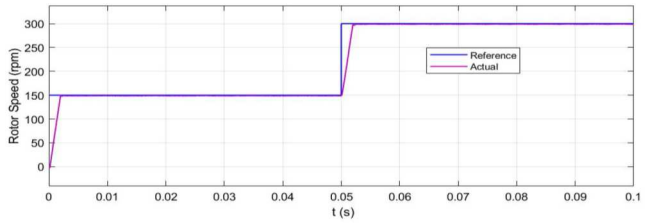

(b)

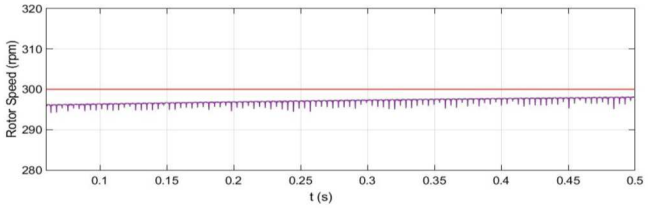

(c)

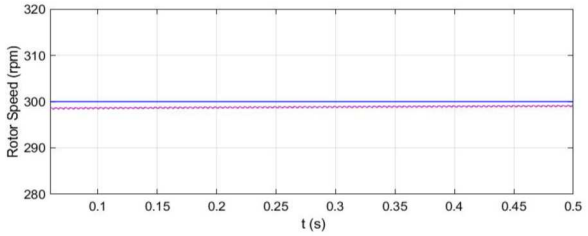

(d)

Fig. 4. The motor speed with the fixed torque: (a) suggested strategy, (b) traditional hystersis current control strategy. (c) zoomed suggested strategy, (d) zoomed traditional strategy.

In Fig. 5 back-EMF of simulated in a, b, c Phases in suggested strategy with the fixed speed of 300 rpm and torque of 5 N.m has been shown. As seen, the back-EMF voltages are trapezoidal.

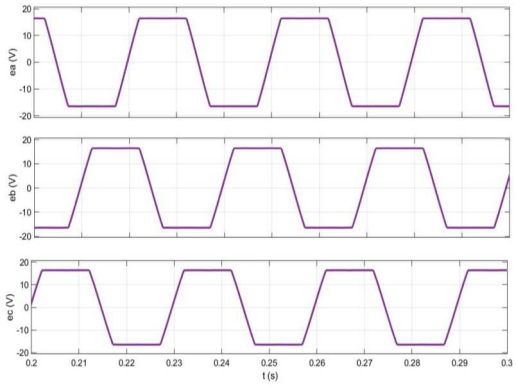

Fig. 5. back-EMF voltage in speed 300 rpm.

The electromagnetic torque of the simulated traditional and suggested strategy with fixed torque and the fixed speed of 300 rpm has been displaced in Fig. 6a and 6b. As seen in figures the torque ripple has declined using the suggested method than traditional method considerably.

TABLE II. SPECIFICATIONSOF OF BLDC MOTOR

Parameter	Value
V_{DC}	60 (V)
Phase Resistance	0.6 (Ω)
Pole Pairs	8
Inertia	0.001(Kg.m^2)
Phase Inductance	1 (mH)
Sampling interval	5(μs)
Linkage flux	0.078125
Speed (rpm)	300
Load Torque	5(N.m)

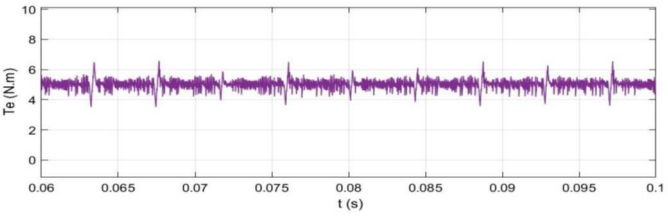

(a)

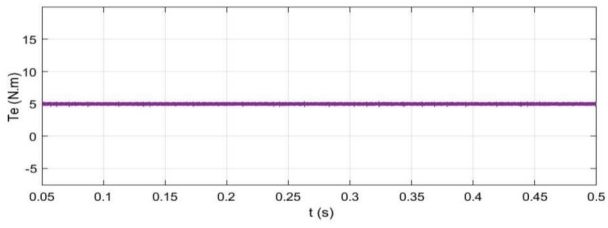

(b)

Fig. 6. Electromagnetic torque: (a) traditional hystersis controller (b) suggested strategy

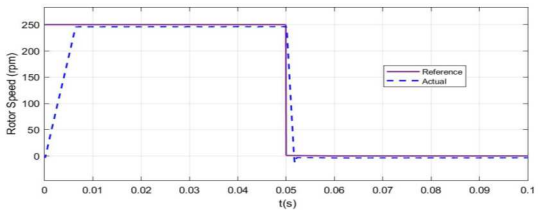

(a)

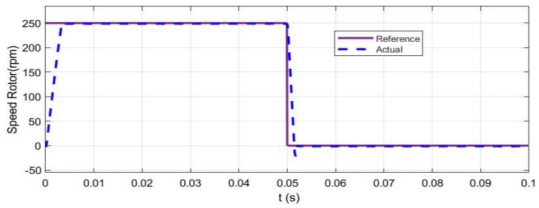

(b)

Fig. 7. Fixed torque in braking state: (a) traditional hystersis current controller (b) suggested controller

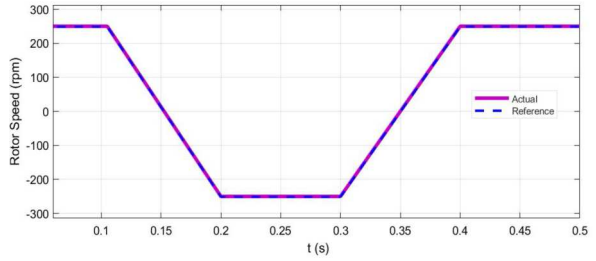

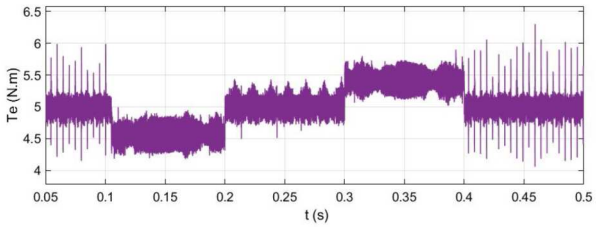

(a)

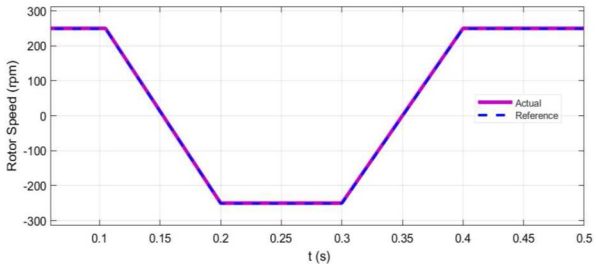

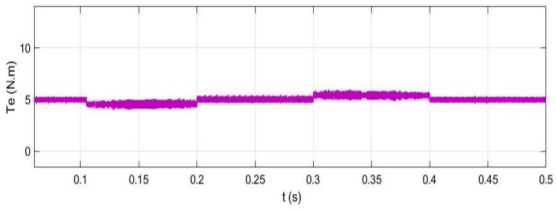

(b)

Fig. 8. Reverse motor direction: (a) traditional hystersis current controller. (b) suggested predictive controller.

It is necessary to assess the performance of the BLDC motor in different working conditions. One of these tests is test during braking state, a speed command is defined in the form of Fig. 7a. Fig. 7a and 7b show speed command is 250 rpm at first and then achieves to zero at fixed load torque. The time takes for the speed to decrease from the reference speed to zero takes about 1ms for the target strategy and 1.3ms for the current hysteresis controller. Table III compares both the predictive and the traditional hysteresis current controller results briefly.

Another test to evaluate the motor is to the direction of reverse rotation that has been performed under full load and rated speed. Using the speed command is reversed rotor direction. Fig. 8a and 8b show the results of this test. As seen, both control methods follow the motor speed of the reference speed, but the suggested ripple method has less torque.

TABLE III. RESULTS COMPARISON OF TWO METHODS

Parameters	**Traditional hysteresis control**	**Suggested MPC**
$\Delta T_{emax}/T_{erated}$	30%	6%
Torque ripple	High	Low
Braking time	1ms	1.3ms
Speed error	4%	1%

V. CONCLUTION

This paper suggests a new model predictive controller for BLDC motor drives without Hall sensors for measuring phase currents and uses of position sensor and calculates back-EMF values. This method reduces torque ripple compared to the hysteresis current control method that is suitable for smooth operations and without noise in in low power industrial applications. Also, the actual speed follows speed reference and error is zero the suggested predictive model controller strategy. As a general conclusion, it can be said that the suggested method is suitable for practical and low power industrial applications.

REFERENCES

[1] H. Jin, G. Liu, H. Li, B. Chen, H. Zhang, "A Fast Commutation Error Correction Method for Sensorless BLDC Motor Considering Rapidly Varying Rotor Speed", IEEE Trans. Ind. Electron., vol. 69, pp. 3938–3947, April 2022.

[2] H. Jin, G. Liu, S. Zheng, "Commutation Error Closed-Loop Correction Method for Sensorless BLDC Motor Using Hardware-Based Floating Phase Back-EMF Integration", IEEE Trans. Ind. Inform. vol. 18, pp. 3978–3986, June 2022.

[3] KT. Chau, Electric Vehicle Machines and Drives, Singapore: John Wiley & Sons, 2015.

[4] T. Shi, Y. Cao, G. Jiang, X. Li, C. Xia, "A torque control strategy for torque ripple reduction of brushless DC motor with nonideal back electromotive force", IEEE Transactions on Ind. Electron., vol. 64, pp. 4423-4433, June 2017.

[5] BN. Kommula, VR. Kota, "A novel scheme for torque ripple minimization of BLDC motor used in solar air conditioner", Electrical Engeenieting, pp. 2473–2483, July 2018.

[6] Y. Cao, T. Shi, X. Li, W. Chen and C. Xia, "A commutation torque ripple suppression strategy for brushless DC motor based on diode assisted buck–boost inverter", IEEE Trans. Power Electron., vol. 34, pp. 5594-5605, June 2019.

[7] M. Taher, A. Halvaei Niasar, S.A. Abbas Taher, "New MPC-based Approach for Torque Ripple Reduction in BLDC Motor Drive", 12th Power Electronics, Drive Systems, and Technologies Conf., Iran, pp. 1–6, February 2021.

[8] M. Moazen , M. Sabahi, “Electric differential for an electric vehicle with four independent driven motors and four wheels steering ability using improved fictitious master synchronization strategy” J. Oper. Authom Power Eng., vol. 2, pp. 141-150, December 2014.

[9] S. B. Ozturk, W. C. Alexander, H. A. Toliyat, “Direct torque control of four-switch brushless dc motor with non-sinusoidal back EMF”, IEEE Trans. Power Electron., vol. 25, pp. 263-271, February 2010.

[10] M. Siami, DA. Khaburi, J. Rodriguez ,“Simplified finite control set-model predictive control for matrix converter-fed PMSM drives”, IEEE Transactions on Power Electronics, vol. 33, pp. 2438-2446, March 2018.

[11] RL. Valle, PMD. Almeida, AA. Ferreira, PG. Barbosa, “Unipolar PWM predictive current-mode control of a variable speed low inductance BLDC motor drive”, IET Electric Power Applications, vol. 11, pp. 688-696, May 2017.

[12] M. Azab,”High performance decoupled active and reactive power control for three-phase grid-tied inverters using model predictive control”, Prot. Control. Mod. Power Syst., July 2021.

[13] M. Azab, “A finite control set model predictive control scheme for single-phase grid-connected inverters”, Renew. Sustain. Energy Rev. vol. 135, January 2021.

[14] AR. Paul, M. George,” Brushless DC motor control using digital PWM techniques”, International Conference on Signal Processing, Communication, Computing and Networking Technologies, India, pp. 733-738, July 2011.

[15] BK. Lee, M. Ehsani, “Advanced Simulation Model for Brushless DC Motor Drives”, Electric Power Components and Systems, vol. 31, pp. 841-868, Jun 2010.

[16] K. Xia, Y. Ye, J. Ni, Y. Wang, P. Xu., “Model Predictive Control Method of Torque Ripple Reduction for BLDC Motor”, IEEE Trans. Magn, vol. 56, pp. 1–6, January 2020.

[17] L.M.A. Caseiro, A.M.S. Mendes, S.M.A. Cruz, “Dynamically Weighted Optimal Switching Vector Model Predictive Control of Power Converters”, IEEE Trans. Ind. Electron., vol. 66, pp. 1235–1245, February 2019